

# Comparison of charge neutralisations of conductors and insulators with corona ionisers

A. Ohsawa

National Institute of Occupational Safety and Health, Japan (JNIOSH)  
1-4-6 Umezono, Kiyose, Tokyo 204-0024, Japan  
phone: (81) 42 491 4512; fax: (81) 42 491 7846  
e-mail: ohsawa@s.jniosh.go.jp

**Abstract**—This paper reports a numerical investigation of phenomena of charge neutralisations of insulators and conductors with the use of a balanced DC or AC ioniser using 2-D cylindrical electrohydrodynamic modelling. The purpose of this study was to examine the difference between the phenomena of the charge neutralisations of conductive and insulating objects on the basis of the motion of ions and to discuss the validity of the standard test method using a conductive plate with regard to its performance and proper applications. We found that the macroscopic ion behaviours with conductive and insulating plates are very similar; however, the early-stage phenomena of the insulator charge neutralisation are complicated and significantly different from the conductor ones, which indicates that the evaluation by the standard test may lead to potential problems in practical applications. In addition, the results of simulations demonstrated that, in the insulator charge neutralisation, ionisers themselves can cause latent hazards during neutralisation, such as a relatively high surface potential for highly electrostatic-sensitive devices and a bipolar surface charge distribution potentially leading to propagating brush discharges, while such situations could not be observed in the conductor neutralisation. We propose proper use of ionisers and the standard test to avoid such hazards.

## I. INTRODUCTION

The electric field resulting from static charge on insulating materials yields electrostatic forces and sometimes initiates electrostatic discharges that can lead to problems and accidents in industry. For example, electrostatic forces attract particulate contaminants or cause materials to stick in undesirable ways; in addition, electrostatic discharges, including those from isolated conductive materials by induction, sometimes result in malfunction of electronic equipment, damage to electronic devices, or occasional fires and explosions. Controlling static charge, therefore, is important to prevent such electrostatic hazards in industry. Charge neutralisation is one of the methods to control the static charge, and corona ionisers are very widely used because of their simplicity.

Thus, the standard technique for testing the performance of an ioniser was developed [1, 2]. The standard test method relies on the use of a charged conductive plate for convenience in testing, including charging it; with this test, the charge decay time and potential at the steady state (offset voltage) are measured under the use of a tested ioniser. In addition, convenient instruments, charged plate monitors, are commercially provided for the test. However, in practice, charged objects to be neutralised by ionisers are insulating materials; therefore, this difference might lead to problems even when using ionisers evaluated to be appropriate for charged conductive materials by the test. Since surface charges on an insulating material are locally neutralised at places that the corresponding polarity of ions reaches during neutralisation, different phenomena of charge neutralisation of insulating materials from those of conductive ones could be expected. In addition, it is difficult to measure the potential and charge on a local surface of insulating materials during charge neutralisation; in particular, the measurement of the local surface charge is impossible when the materials are thin and their opposite side surface is also charged. In this study, therefore, we numerically investigate the difference of the charge neutralisations of conductors and insulators with ionisers.

Despite the widespread use of ionisers, the understanding of the phenomena of charge neutralisation using ionisers strongly depends on empirical knowledge. Many experimental investigations [3–11] have been carried out by measuring the potential or current of a charged metal plate during neutralisation; however, in such investigations, only resultant phenomena by ion behaviour could be measured. To understand the essential features of charge neutralisation, the investigation of the motion of ions is of great importance. In addition, the manufacture of recent electrostatic-sensitive devices in electronic industries requires more precise neutralisation. Therefore, understanding based on theoretical approaches involving ion behaviour will result in better neutralisation. An electrohydrodynamic model that can solve the self-consistent motion of ions is very useful for this purpose. In our previous studies, a one-dimensional ion fluid model [12, 13] was used and demonstrated that the essential conditions for sufficient neutralisation with AC ionisers with air blowing are that, in the region of ion transport, the density distributions of positive and negative ions have less fluctuation and their charges are quasi-neutralised at the steady state, resulting in a small fluctuation in the offset voltage. Furthermore, in the tube transport of ions, we also demonstrated that a quasi-neutralised ion charge distribution (a charge distribution in which the density distributions of the positive and negative ions are the same) created in the tube greatly reduces the radial electric field, resulting in an extremely decreased loss of ions at the tube wall using 2-D fluid simulations with assuming laminar airflow in the tube [14]. In addition, it was found that the formation of such ion charge distributions greatly depends on the relationship between the frequency of the corona discharge and the airflow velocity. Furthermore, results from the investigation of the production and minimisation of the offset voltage using a two-dimensional electrohydrodynamic model demonstrated that the emission of continuously balanced ions from ionisers can make the offset voltage zero independently of the placement of an object to be neutralised and the air blower velocity used for ionisers [15].

In this paper, the 2-D electrohydrodynamic model is used to compare the phenomena of the charge neutralisations of conductive and insulating materials with a DC or AC ioniser with an emphasis on the investigation of ion behaviour during neutralisation, and the valid-

ity of the standard test method using a conductive plate is discussed.

## II. MODEL

A 2-D electrohydrodynamic model used in this paper is the same as one used previously [15] for the charge neutralisation of a conductive object. The model is described in detail in [15], and will thus be only briefly discussed here except for the model for an insulating object. The 2-D electrohydrodynamic model solves self-consistent motion of positive and negative ions, and the governing equations consist of the equations of incompressible fluid for airflow, the continuity equations for positive and negative ions, and Poisson's equation, as follows;

$$\nabla \cdot \mathbf{v}_a = 0, \quad (1)$$

for airflow velocities, which is reduced from the mass conservation equation. The momentum conservation equation of air fluid flow is,

$$\rho_a \frac{\partial \mathbf{v}_a}{\partial t} + \rho_a (\mathbf{v}_a \cdot \nabla) \mathbf{v}_a = -\nabla P + \mathbf{F}_E + \nabla \cdot (\mu \nabla \mathbf{v}_a), \quad (2)$$

in which electric force density  $\mathbf{F}_E = e(n_p - n_n)\mathbf{E}$  by the space charge of ions is included. Here,  $\mathbf{v}_a$ ,  $\rho_a$ ,  $P$ , and  $\mu$  are the airflow velocity, mass density of air, pressure, and viscosity coefficient, respectively. The motion of positive and negative ions is expressed by the following continuity equations,

$$\frac{\partial n_p}{\partial t} + \nabla \cdot (n_p \mathbf{v}_p) - D_p \nabla^2 n_p = -\beta n_p n_n, \quad (3)$$

for positive ions and

$$\frac{\partial n_n}{\partial t} + \nabla \cdot (n_n \mathbf{v}_n) - D_n \nabla^2 n_n = -\beta n_p n_n, \quad (4)$$

for negative ions, where  $n_p$  and  $n_n$  are the positive and negative ion densities, respectively, and  $\mathbf{v}_p = \mathbf{w}_p + \mathbf{v}_a$ ,  $\mathbf{v}_n = \mathbf{w}_n + \mathbf{v}_a$ ,  $\mathbf{w}_p$  and  $\mathbf{w}_n$  are the corresponding drift velocities, respectively. The symbols  $D$  and  $\beta$  denote the diffusion and ion-ion recombination coefficients, respectively. We use the mobilities for the positive and negative ions and the recombination coefficient in air given by Morrow and Lowke [16] and the diffusion coefficients in [17]. To obtain the electric field, the Poisson's equation,

$$\nabla^2 \phi = -e(n_p - n_n)/\epsilon_0, \quad (5)$$

and

$$\mathbf{E} = -\nabla \phi, \quad (6)$$

are used. Here,  $e$  is the elementary charge (ion charge),  $\epsilon_0$  is the electric constant,  $\mathbf{E}$  is the electric field, and  $\phi$  is the potential. For an insulating object to be neutralised, the potential inside the object is obtained from,

$$\nabla^2 \phi = 0, \quad (7)$$

and the boundary condition at the interface of the insulating object,

$$\mathbf{n} \cdot (\mathbf{D}_0 - \mathbf{D}_1) = \sigma_s, \quad (8)$$

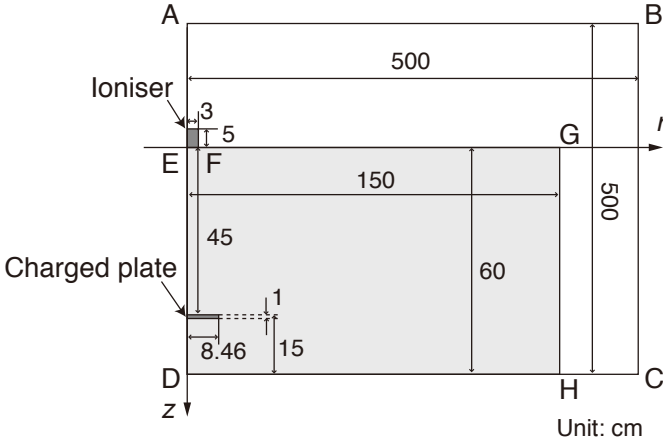


Fig. 1. Computational domains of the model.

is used, where  $\mathbf{n}$  is the outwardly directed unit vector normal to the interface and  $\mathbf{D}_0$  and  $\mathbf{D}_1$  are the displacements of outside and inside at the surface of the insulating object, respectively. The relative electric permittivity of the insulating object is 2.0.

The geometry of an ioniser and a charged object (plate) used in the standard test method for overhead ionisers [1, 2] is modelled in two-dimensional, axisymmetric cylindrical coordinates  $(r, z)$ , as shown in Fig. 1. The origin point of  $(r, z)$  is point E. To employ the coordinate system, the shapes of the ioniser and the charged plate are assumed to be circular disks with a diameter of 6 cm and thickness of 5 cm for the ioniser and a radius,  $R_{cp}$ , of 8.64 cm and thickness of 1 cm for the charged plate. The separation between them is 45 cm, and the charged plate is placed at 15 cm above a grounded plane according to the test method.

Poisson's equation, Eq. (5), was solved throughout the entire computational domain, ABCD, and the equations for air fluid flow and ions are solved only in region EGHD, shown in Fig. 1. The potential on the boundary of ABCD is assumed to be zero except on the axis. The body of the ioniser, including the conductive grid generally used for its ion outlet, is grounded. The radial electric field on the axis is zero. In the computational domain for solving Eqs. (1)–(4) for airflow and ions of region EGHD, the following boundary conditions are assumed, where the symbols of  $u$  and  $v$  denote the velocities of the components of the  $r$  and  $z$  directions, respectively: at boundary FG, the gradients of the velocities of airflow are assumed to be zero, i.e.,  $\partial u_a / \partial z = \partial v_a / \partial z = 0$ , and the gradients of ion densities are assumed to be zero,  $\partial n_p / \partial z = \partial n_n / \partial z = 0$ ; at boundary GH,  $\partial u_a / \partial r = \partial v_a / \partial r = 0$  for airflow and  $\partial n_p / \partial r = \partial n_n / \partial r = 0$  for positive and negative ions; at boundary DH on the grounded plane,  $u_a = v_a = 0$  and  $n_p = n_n = 0$ ; at the axis boundary, ED,  $u_a = 0$  and  $\partial v_a / \partial r = 0$  for airflow and  $u_p = u_n = 0$  for ions; at the boundary of the ioniser, EF,  $u_a = 0$  and  $v_a$  is set to an initial velocity,  $v_{a0}$ , from an air blower of the ioniser, and the densities,  $n_{p0}$  and  $n_{n0}$ , of positive and negative ions, respectively, emitted from the ioniser, are set to those shown in Fig. 2, where, for AC ionisers, they are calculated on the basis of the

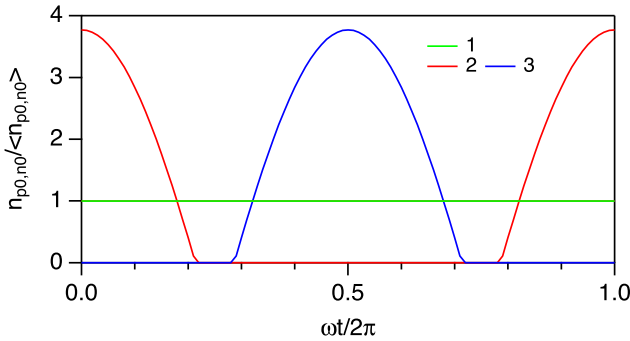


Fig. 2. Densities of positive and negative ions emitted from ionisers used in this investigation. 1: those of a balanced DC ioniser, 2, 3: those for positive and negative ions of a balanced AC ioniser, respectively.

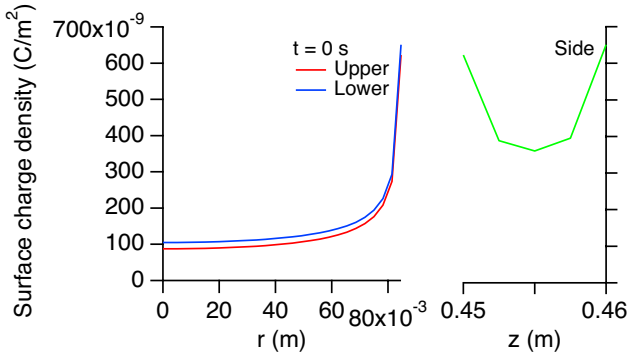


Fig. 3. Initial surface charge density distribution of the insulating plate.

ion source model [12]. Here, angle brackets  $\langle \rangle$  denote their time average values, and the function of the applied voltage for corona discharges with the frequency of 50 Hz in the AC ioniser is assumed to be cosine. At the boundary on the surface of the charged plate,  $u_a = v_a = 0$  and  $n_p = n_n = 0$ , and the charges of ions reaching the charged plate are assumed to be transferred to the surface charges on it. The potential,  $\phi_{cp}$ , of the charged plate is initially set to 1.2 kV at time  $t = 0$  s. The initial distribution of the surface charge density,  $\sigma_s$ , of the insulating plate modelled is calculated from  $\sigma_s = \epsilon_0 E_s$ , as shown in Fig. 3, where  $E_s$  is the outwardly directed electric field normal to the surface of the conductive plate of 1.2 kV; thus, the distribution of the initial surface potential of the insulating plate is the same as that of the conductive one. The capacitance,  $C_{cp}$ , of the conductive plate is 20 pF according to the standard test method.

To obtain the potential of the conductive plate during neutralisation, we applied a circuit equation according to which the net current in the system is equal to the current of the capacitance of the plate, expressed by Eq. (9). The net current of the left-hand side of this equation is obtained from Morrow and Sato's equation [18], which, consequently, accounts

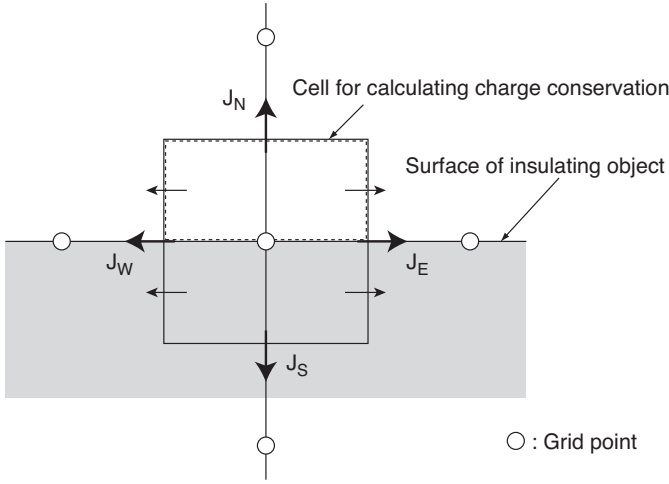


Fig. 4. A cell for calculating the conservation of charge at a local surface of insulating object.

for the displacement current by the motion of ions.

$$e \int_V (n_p \mathbf{v}_p - n_n \mathbf{v}_n - D_p \nabla n_p + D_n \nabla n_n) \cdot \mathbf{e}_L dv = -C_{cp} \frac{d\phi_{cp}}{dt}, \quad (9)$$

where  $v$  is the volume of the system and  $\mathbf{e}_L$  is the Laplace field when unit voltage is applied to the plate.

For the insulating plate, the conservation of charge in a cell at a local surface of the insulating object is used to obtain the surface charges on the plate,  $\sigma_s$ , during neutralisation, as shown in Fig. 4.

$$\int_S \mathbf{J} \cdot \mathbf{n} dS = - \int_{v_c} \frac{d\rho_c}{dt} dv_c = - \left( \int_s \frac{d\sigma_s}{dt} ds + \int_{v_{ca}} \frac{d\rho_{ca}}{dt} dv_{ca} \right), \quad (10)$$

where  $S$  is the surface area of the cell,  $\mathbf{J}$  is the vector of current density,  $\mathbf{n}$  is the outwardly directed unit vector normal to the surface of the insulating object,  $v_c$  is the volume of the cell,  $\rho_c$  is the charge density in the cell,  $s$  is the surface area of the insulating object in the cell, and  $v_{ca}$  is the volume of the air space in the cell. Here, the volume integration of the charge density,  $\rho_c$ , includes the charge in the air space above the insulator surface, shown as a dashed rectangle in Fig. 4; therefore, the volume integration of this charge density,  $\rho_{ca}$ , is added in Eq. (10). In addition, for the current density,  $\mathbf{J}$ , not only the conduction current of ions but also the displacement current is considered. The surface resistivity of the insulating plate is assumed to be infinity for modelling an ideal insulator; thus, the conduction of the surface charge via the surface resistance is ignored.

Equations (1) and (2) for air fluid flow were solved using the Highly Simplified Marker-and-Cell (HSMAC) method [19]. The continuity equations for ions of Eqs. (3) and (4) were solved with the second-order Runge-Kutta time evolution, and the flux-corrected transport

(FCT) scheme [20, 21] was used in the terms of convections (the second terms of the left-hand sides) of these equations. For solving Poisson's equation of Eqs. (5) and (7), the successive over-relaxation (SOR) method [22] was used.

Dynamic spatial grids were used for solving the governing equations, in which, at the region of  $r \leq 2R_{cp}$ , the grids are finer (much finer around the plate), and, at the region far from the ioniser and charged plate, coarser grids that increase and decrease exponentially were used. Since the grid with staggered points of velocities for the air fluid flow is different from other grids, a linear interpolation with volume weighting from the values on the four nearest grid points [23] is used for obtaining  $\mathbf{F}_E$  in Eq. (2) and  $\mathbf{v}_a$  used in Eqs. (3) and (4). A dynamic time-step satisfying the Courant-Friedrichs-Lewy (CFL) condition is used, where, for AC ionisers, the maximum of the time-step is one-fiftieth of a cycle of 50 Hz for their corona discharges.

### III. RESULTS AND DISCUSSION

Simulations of charge neutralisations of conductive and insulating plates were carried out for balanced DC and AC ionisers with  $\langle n_{p0} \rangle = \langle n_{n0} \rangle = 1 \times 10^{14} \text{ m}^{-3}$  and  $v_{a0} = 3.0 \text{ m/s}$  in this investigation. The results of the charge neutralisation of conductive plates with DC, AC and pulse-DC ionisers are discussed in [15] in detail with the emphasis on the production and minimisation of the offset voltage. The distributions of the surface potentials of the conductive and insulating plates are initially the same to compare the phenomena during neutralisation between them. For this purpose, the distribution of the initial surface charge density of the insulating plate is set to that shown in Fig. 3; furthermore, simulations with the capacitance of the conductive plate of 8.2 pF corresponding to that of the conductive plate itself, which is numerically calculated, were carried out for an exact comparison in addition to simulations with the capacitance of 20 pF used in the standard test because the capacitance of 20 pF could lead to a longer decay and a lower fluctuation of the potential of the plate than those with the conductive plate itself.

Here, to investigate the local surface potential and charge on the insulating plate during neutralisation as their representative values, those of the centres of the upper, lower, and side surfaces of the plate, in addition to the averaged values over the surface area of the plate, are plotted in figures.

The potential decays of the conductive and insulating plates with the balanced DC ioniser are comparable, as shown in Fig. 5, while the decay of the conductive plate of 20 pF used in the standard test, which includes the excess capacitance, as described above, is the slowest. On this point, the standard test could measure the worst decay time. For the insulating plate, the potential decay on the upper surface is faster than the lower one because the lower side can be neutralised by ions moving towards the lower side after passing the upper surface. In addition, it is of interest that the potential decay of the side surface of the plate is faster than that of other surfaces and similar to that of the conductive plate of 8.2 pF.

Since the ions emitted from the DC ioniser are continuously balanced, they can yield a quasi-neutralised ion charge distribution in the entire space at the steady state, resulting in that the offset voltage of the conductive plate is approximately zero [15], as shown in Fig. 6. For the insulating plate, however, the potentials on the plate become relatively large

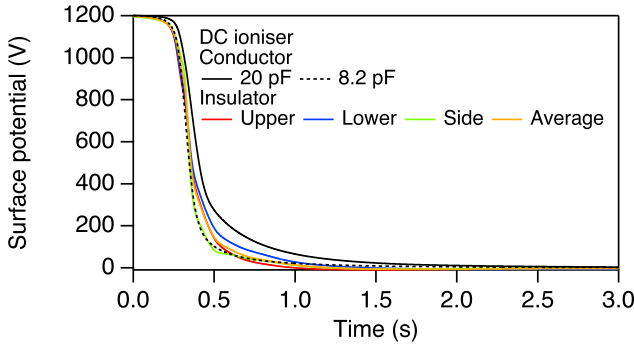


Fig. 5. Potential decays of the conductive and insulating plates with the balanced DC ioniser with  $n_{p0} = n_{n0} = 1.0 \times 10^{14} \text{ m}^{-3}$  and  $v_{d0} = 3.0 \text{ m/s}$ .

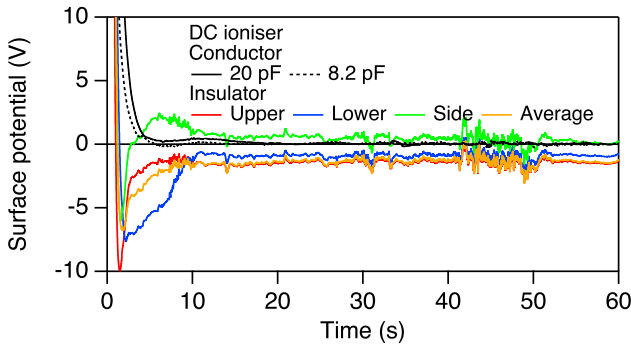


Fig. 6. Offset voltages of the conductive and insulating plates with the balanced DC ioniser.

negative values at once ( $t < 10 \text{ s}$ ), and, at the steady state, the potentials have certain values of non-zero and sometimes include fluctuations. The potentials on the insulating plate at the steady state are within  $\pm 10 \text{ V}$ , which leads to no hazardous situations for general electrostatic-sensitive devices, while, at the early stage of neutralisation ( $t < 10 \text{ s}$ ), the potentials are over  $\pm 5 \text{ V}$ , which potentially leads to problems for more sensitive devices, e.g., magneto-resistive heads, even when the potential of the conductive plate reached within  $\pm 5 \text{ V}$ . Regarding this point, the evaluation of the performance of an ioniser by the standard test using a conductive plate might lead to a latent problem in practical applications. This indicates that, for appropriate application of the standard test to the neutralisation of insulating objects, sufficient neutralisation time may be required; for example, the required neutralisation time must at least be several tens of times the decay time (the time required for the potential of the conductive plate to decay from  $\pm 1000 \text{ V}$  to  $\pm 100 \text{ V}$ ) measured with the standard test.

The time variation of the surface charge densities on the insulating plate during neutralisation with a balanced DC ioniser, in which bipolar charge distributions on the surface



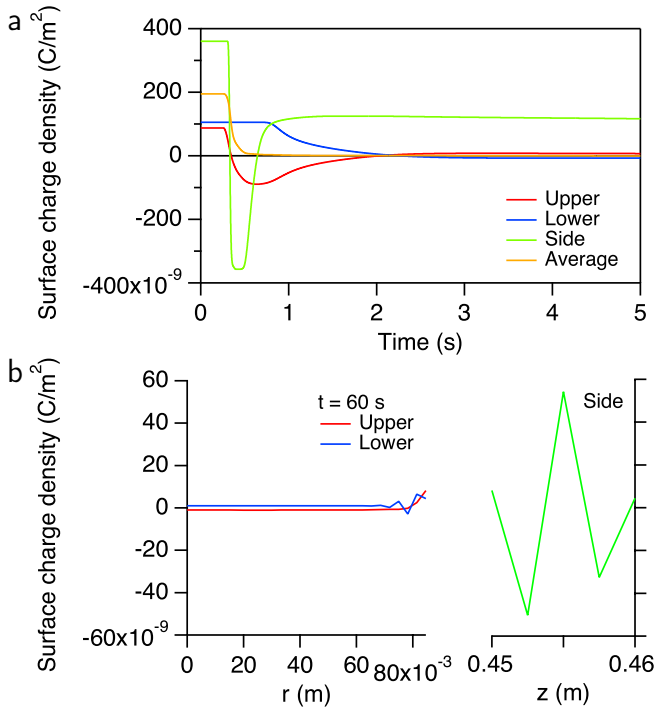


Fig. 7. Surface charge densities on the insulating plate during neutralisation with the balanced DC ioniser, a: their time variation in initial period, and b: the surface charge distribution at  $t = 60.0$  s.

are observed, is complicated, as shown in Fig. 7. At the early stage of the charge neutralisation ( $t < 1.0$  s), strong over-neutralisations having negative charge occur at the upper and side surfaces due to the electric field by the surface charges on the lower side surface where no ions reach at this time; thus, the corresponding negative surface potentials appear in Fig. 6. In addition, the polarity of the upper and lower surface charges is reversed at  $t = 2.2$  s. Furthermore, as shown in Fig. 7a, the surface charges on the side surface are difficult to be neutralised. As a result, as shown in Fig. 7b, relatively high charge densities on the side surface with a very slow decrease are observed even when the plate is sufficiently neutralised at  $t = 60.0$  s. The charge distribution on the side surface, however, is bipolar, resulting in a small surface potential with the averaged potential of  $-1.7$  V at the side surface. Therefore, macroscopically, the surface charges on the plate are considered to be sufficiently neutralised. The phenomena of this neutralisation will be discussed in detail later on the basis of the motion of ions.

The corresponding motion of ions during neutralisation of the conductive and insulating plates with the balanced DC ioniser is shown in Fig. 8. The plates are initially positively charged; thus, the negative ions move towards the plates faster, and then, the positive ions reach the plates. The profiles of the main flows of positive and negative ions for the conductive and insulating plates, which have ion density  $> 10^{12}$  m<sup>-3</sup> and are mainly transported by airflow, are very similar, while the portions of the positive and negative ions from the

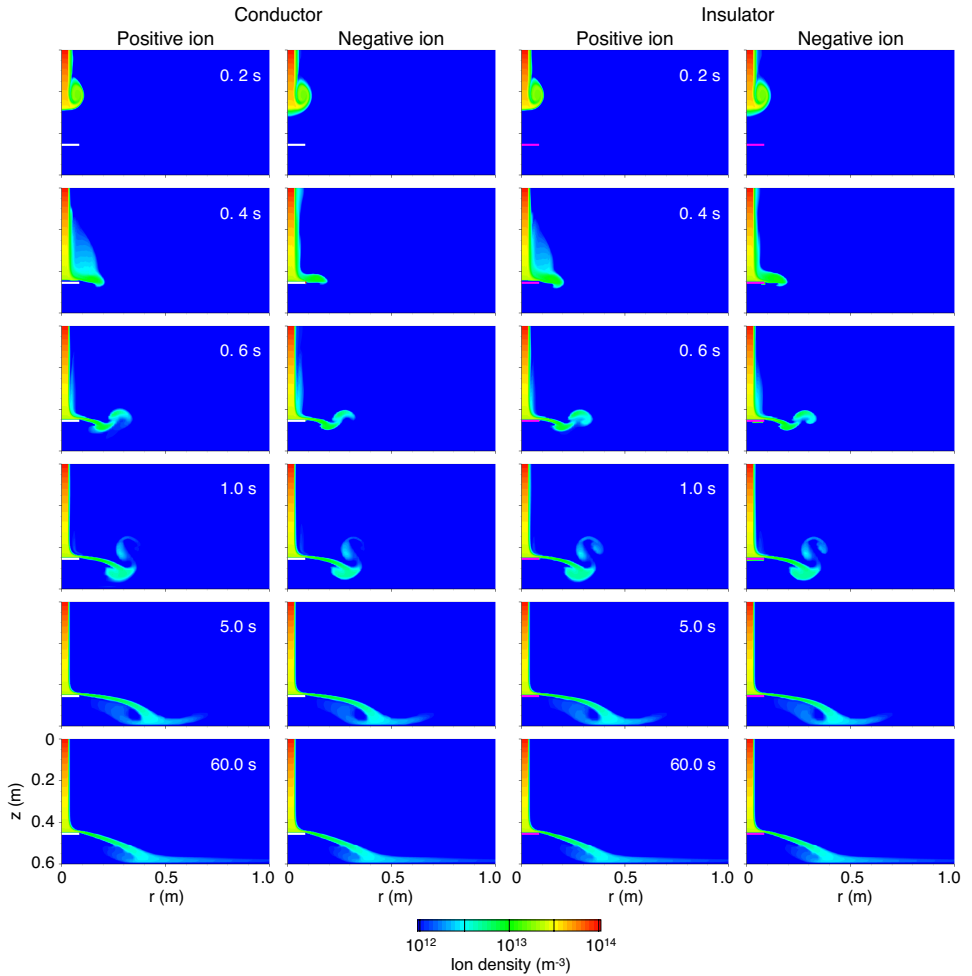


Fig. 8. Time evolution of the density distributions of positive and negative ions during neutralisation for the conductive and insulating plates with the balanced DC ioniser with  $n_{p0} = n_{n0} = 1.0 \times 10^{14} \text{ m}^{-3}$  and  $v_{a0} = 3.0 \text{ m/s}$ .

main flows move towards the insulating plate. Finally, the density distributions of the positive and negative ions for both the conductive and insulating plates create quasi-neutralised ion charge distributions in the entire space at the steady state. We demonstrated that the quasi-neutralised charge distribution can yield approximately zero offset voltage for the conductive plates [15]. For the insulating plate, however, small surface potentials within a few volts remain (Fig. 6) due to the surface charges shown in Fig. 7b, which cannot be eliminated.

To investigate the initial stage of the charge neutralisation of the insulating plate, enlarged plots of the ion density distributions around the plate with a colour level having a

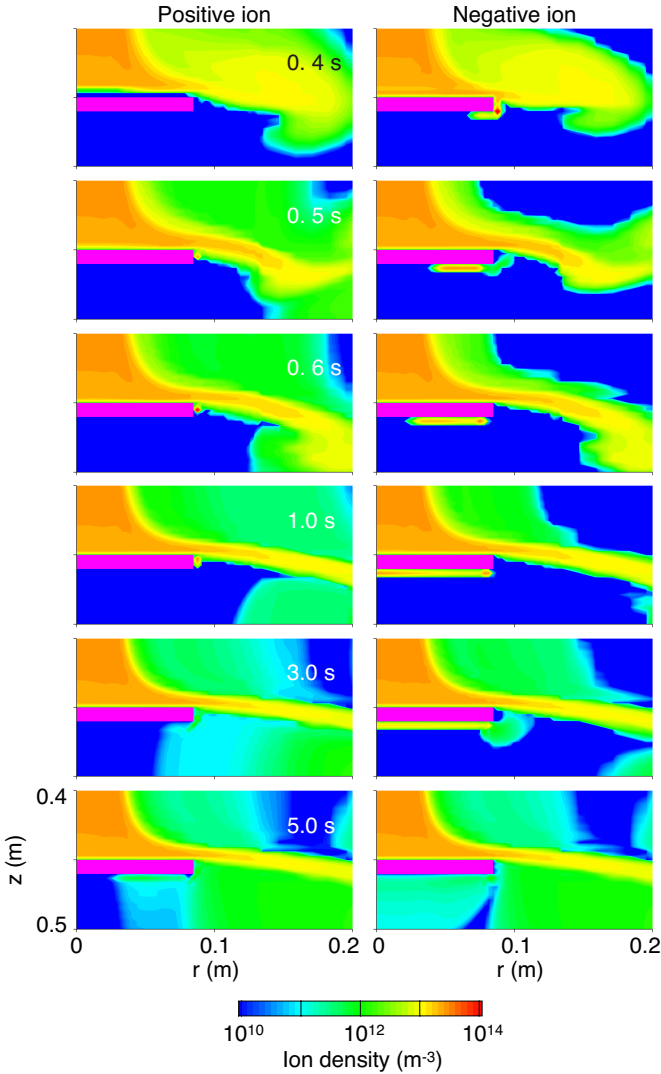


Fig. 9. Enlarged plots of the density distributions of positive and negative ions during neutralisation of the insulating plate (purple rectangle) with the balanced DC ioniser with  $n_{p0} = n_{n0} = 1.0 \times 10^{14} \text{ m}^{-3}$  and  $v_{a0} = 3.0 \text{ m/s}$ .

wider range of ion density of  $10^{10} - 10^{14} \text{ m}^{-3}$  are shown in Fig. 9. Since the charge of the plate is initially set to positive in this investigation, the negative ions reach the upper surface of the plate faster, as shown in plots at  $t = 0.4 \text{ s}$  in Fig. 9. Thus, the neutralisation of the charges on the upper surface begins first, and then, charge neutralisation on the side of the plate starts. Due to the positive charges of the lower side of the plate, these charges on the upper and side surfaces are over-neutralised, resulting at once in negative surface

charges during neutralisation, as shown in Fig. 7a. The over-neutralised negative surface charges take place to reduce the influence of the electric field by the charges of the lower surface on the electric fields at the upper and side surfaces. After this, the positive ions also reach the upper surface of the plate by the forced airflow; in addition, the over-neutralised negative charges on the upper and side surfaces attract nearby positive ions; on the other hand, the negative ions move away from the side surface and move towards the lower side surface along the surface due to the electric fields created by the surface charges, where their negative ions are transported from the main flow, as shown in plots at  $t = 0.5$  s in Fig. 9. Consequently, after this, the over-neutralised negative charges on the upper and side surface decrease, as shown in Fig. 7a. Furthermore, the negative ions that moved towards the lower surface are isolated and then extend along the lower surface, as shown in plots at  $t = 0.6$  and  $1.0$  s in Fig. 9; however, the positive ions still remain at the side surface because the averaged charge with bipolar charges at the side wall is still negative. Moreover, excess negative ions at the lower side surface go back to the main flow; at this time, the portion of the positive ions also moves towards the lower side surface, as shown in plots at  $t = 3.0$  s in Fig. 9. The positive ions at the lower side surface then extend towards the centre along the surface, and the negative ions at the lower side gradually move away from the plate, as shown in plots at  $t = 5.0$  s in Fig. 9. Thus, such motions of the positive and negative ions during neutralisation result in the time variation of the surface charge densities, as shown in Fig. 7a. In addition, when the positive ions exist near the side surface, their density is higher near the centre of the side surface, as shown in plots at  $t = 0.5, 0.6,$  and  $1.0$  s in Fig. 9; on the other hand, when the negative ions exist near the side surface, as shown in plots at  $t = 0.4$  s in Fig. 9, their density is lower near the centre of the side surface due to resultant electric fields by nearby surface charges, resulting in a bipolar surface charge distribution there. The bipolar surface charges created at the side surface in the early stage of the neutralisation are kept during neutralisation, while their absolute values decrease very slowly. This is because the influence of the electric fields created by the bipolar surface charges is almost eliminated at a few millimetres from the plate; thus, it is difficult to neutralise the bipolar charges created by charges on the neighbouring surfaces even when ions exist near the plate.

Since the initial surface charges were not high, the over-neutralised charges with a bipolar charge distribution led to no hazardous situation. The result, however, indicates that ionisers have potential hazards to yields a highly charged bipolar distribution with different polarity on the upper and lower surfaces. The distribution could initiate a propagating brush discharge that could lead to an ignition at the early stage of charge neutralisation if the initial charges are higher and the plate thinner. Such a situation is possible when charged objects are moving, e.g., continuously entrained products or long films with relatively fast transportation, because sufficient neutralisation time is not given. Furthermore, when objects are much wider, ions are difficult to be transported to the lower side surface; therefore, the hazardous bipolar charge could be maintained longer. To avoid this, ionisers placed at both the upper and lower sides, which simultaneously neutralise the individual surface charges, would be necessary when both side surfaces of an insulating object are charged.

The phenomena of the charge neutralisations of conductive and insulating plates with a balanced AC ioniser are almost identical to those with the balanced DC ioniser, except for

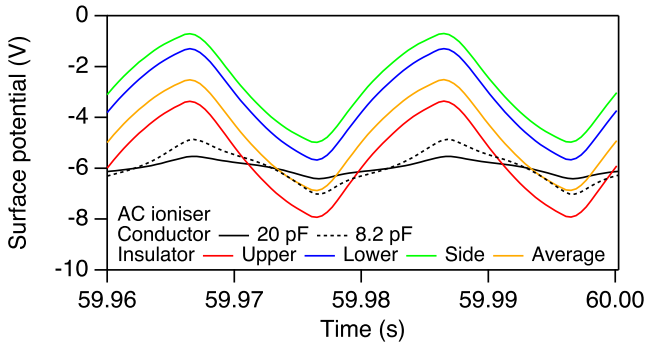


Fig. 10. Steady-state surface potentials on the conductive and insulating plates with the balanced AC ioniser with  $\langle n_{p0} \rangle = \langle n_{n0} \rangle = 1.0 \times 10^{14} \text{ m}^{-3}$  and  $v_{a0} = 3.0 \text{ m/s}$ .

the surface potentials of the plates having negative values with the oscillation of 50 Hz at the steady state, as shown in Fig. 10. The oscillated negative offset voltage of the conductive plate is caused by mono-polar space charges of positive or negative ions alternately created near the ioniser outlet that lead to imbalance between positive and negative ion currents as well as a relatively high space potential of positive or negative value alternately created near the ioniser [15]. Here, the creation of the mono-polar space charges near the ioniser is caused by ions emitted from the AC ioniser. Similarly, the surface potentials on the insulating plate have negative values with oscillation of 50 Hz. In addition, the oscillation of the surface charge densities is approximately  $10 \text{ pC/m}^2$ . It is of interest that the amplitude of the oscillation is several times larger than that of the conductive plate and sometimes over  $\pm 5 \text{ V}$ , even with sufficient neutralisation time. This indicates that the equivalent capacitance of the insulating plate with the resultant surface charge density distribution at the steady state seems to be smaller than that of the conductive one. Therefore, the standard test method using a conductive plate with a capacitance of  $20 \text{ pF}$  for the evaluation of the performance of AC ionisers might lead to a potential problem.

Consequently, balanced DC ionisers enabling the offset voltage to be zero for conductive plates seem to be more appropriate than balanced AC ones for highly electrostatic-sensitive devices, while we proposed a method, a continuously balanced AC ioniser, that can eliminate the offset voltage of conductive plates as well as its AC oscillation [15].

Work in progress is the investigation of insulator charge neutralisation using simulations with different distributions of the initial surface charge density on the insulating plate.

#### IV. CONCLUSION

We investigated the difference between the phenomena of the charge neutralisations of conductive and insulating plates with balanced DC and AC ionisers using 2-D electrohydrodynamic modelling. The macroscopic ion behaviours with the conductive and insulating plates were almost the same; in particular, with sufficiently neutralised plates at the steady state, the density distributions of ions for the conductive and insulating plates be-

came identical. As a result, we found that the evaluation of ionisers by the standard test using a conductive plate is likely to present no obstacles for general applications and ordinary electrostatic-sensitive devices. For the insulating plate, however, the portions of the positive and negative ions are transported to the plate to neutralise the surface charges on it at the early stage of neutralisation. At this time, very complicated surface charge distributions were created on the plate due to resultant electric fields by the surface charges themselves; in addition, relatively high surface potentials and charge densities, which may cause potential problems and hazards, were observed during neutralisation. Since such phenomena could not be observed for the conductive plate, the results suggest that the evaluation of ionisers by the standard test could lead to a latent problem in practical applications, in particular, for highly sensitive devices. In addition, a bipolar charge distribution having different polarity at the upper and lower surfaces of the plate, which can potentially lead to propagating brush discharges, was observed at the early stage of neutralisation. This indicates that ionisers themselves could create a hazardous situation resulting in ignition when the initial surface charges are higher and the object to be neutralised is thinner. Furthermore, we found that a local bipolar charge distribution on the insulating plate, which cannot be eliminated, is created at the steady state.

#### ACKNOWLEDGMENTS

The author would like to thank Dr. Richard Morrow and Professor Mikio Ohuchi for their helpful discussions during this research. This work was supported by JSPS Grant-in-Aid Scientific Research (C-23510214).

#### REFERENCES

- [1] IEC 61340-5-1, Electrostatics – Part 5-1: Protection of electronic devices from electrostatic phenomena – General requirements, 1988.
- [2] ANSI/ESD STM3.1-2006, For the protection of electrostatic discharge susceptible items – Ionization, ESD Association, 2006.
- [3] L. Levit, A. Wallash, Measurement of the effects of ionizer imbalance and proximity to ground in MR head handling, *J. Electrostat.* 47 (1999) 305–313.
- [4] J.-S. Chang, K.G. Harasym, P.C. Looy, A.A. Berezin, Neutralisation of static surface charges by an ac ionizer in a nitrogen environment, *Inst. Phys. Conf. Ser. No. 163* (1999) 289–294.
- [5] C.G. Noll, Balanced static elimination in variable ion mobility environments, *J. Electrostat.* 49 (2001) 169–194.
- [6] J.-S. Chang, A.A. Berezin, Neutralization of static surface charges by a flow stabilized corona discharge ionizer in a in a nitrogen environment, *J. Electrostat.* 51–52 (2001) 64–70.
- [7] J.-S. Chang, A.A. Berezin, C.G Noll, Neutralization of static surface charges by an ac ionizer in a nitrogen and dry air environment, *J. Appl. Phys.* 91 (2002) 1020–1025.
- [8] C.G. Noll, Temperature dependence of dc corona and charge-carrier entrainment in a gas flow channel, *J. Electrostat.* 54 (2002) 245–270.

- [9] C.G. Noll, Charge-carrier extraction from air and nitrogen gas streams that entrain charge from dc corona ionizers, *J. Electrostat.* 54 (2002) 271–282.
- [10] J.M. Crowley, D. Leri, G. Dahlhoff, L. Levit, Equivalent circuits for air ionizers used in static control, *J. Electrostat.* 61 (2004) 71–83.
- [11] J.M. Crowley, A. Ignatenko, L.B. Levit, Biased-plate characterization of pulsed DC ionizers, *J. Electrostat.* 62 (2004) 219–230.
- [12] A. Ohsawa, Modeling of charge neutralization by ionizer, *J. Electrostat.* 63 (2005) 767–773.
- [13] A. Ohsawa, Efficient charge neutralization with an ac corona ionizer, *J. Electrostat.* 65 (2007) 598–606.
- [14] A. Ohsawa, In-tube transport of ions for charge neutralization, *J. Phys. Conf. Ser.* 142 (2008) 012014-1-4.
- [15] A. Ohsawa, 2-D electrohydrodynamic simulations towards zero offset voltage with corona ionisers, Manuscript submitted for publication.
- [16] R. Morrow, J.J. Lowke, Streamer propagation in air, *J. Phys. D: Appl. Phys.* 30 (1997) 614–627.
- [17] K. Honda, *Gas Discharge Phenomena*, Tokyo Denki University Press, Tokyo, 1988 (in Japanese).
- [18] R. Morrow, N. Sato, The discharge current induced by the motion of charged particles in time-dependent electric fields; Sato's equation extended, *J. Phys. D: Appl. Phys.* 32 (1999) L20–L22.
- [19] C.W. Hirt, J.L. Cook, Calculating three-dimensional flows around structures and over rough terrain, *J. Comput. Phys.* 10 (1972) 324–340.
- [20] S.T. Zalesak, Fully multidimensional flux-corrected transport algorithms for fluids, *J. Comput. Phys.* 31 (1979) 335–362.
- [21] C.R. DeVore, An improved limiter for multidimensional flux-corrected transport, NRL/MR/6440-98-8330, Naval Research Laboratory, (1998).
- [22] W.H. Press, S.A. Teukolsky, W.T. Vetterling, B.P. Flannery, *Numerical recipes in C*, 2nd ed., Cambridge Univ. Press, 1992.
- [23] C.K. Birdsall, A.B. Langdon, *Plasma Physics via Computer Simulation*, McGraw-Hill, 1992.